



# Target immobilization on glass microfiber membranes as a label-free strategy for hit identification

Yinan Wang<sup>1</sup> · Yan He<sup>1</sup> · Xiaojiao Ye<sup>1</sup> · Yixiao Zhang<sup>1</sup> · Xiuxiu Huang<sup>1</sup> · Hongli Liu<sup>1</sup> · Wenqing Dong<sup>1</sup> · Dongzhi Yang<sup>1</sup> · Dong Guo<sup>1</sup>

Received: 22 July 2023 / Revised: 9 September 2023 / Accepted: 12 September 2023 / Published online: 21 September 2023  
© The Author(s), under exclusive licence to Springer-Verlag GmbH, DE part of Springer Nature 2023

## Abstract

The discovery of novel chemical entities targeting G protein-coupled receptors (GPCRs) is usually guided by their receptor affinity. However, traditional affinity assay methods and hit identification procedures are usually laborious and expensive. In this work, the type-2 vasopressin receptor (V<sub>2</sub>R) was chosen as a prototypical GPCR. Membrane fragments from cells highly expressing SNAP-V<sub>2</sub>R were immobilized on the surface of a glass microfiber (GMF) coated with O<sup>6</sup>-benzylguanine (BG). This was achieved by transferring the benzyl group of BG to the active site of the SNAP-tag through a nucleophilic substitution reaction. As a result, a biofilm called SNAP-V<sub>2</sub>R@GMF-BG was produced that showed good specificity and stability. The adsorption ratio for each V<sub>2</sub>R ligand treated with SNAP-V<sub>2</sub>R@GMF-BG was determined by HPLC and exhibited a good linear correlation with the K<sub>i</sub> value determined by displacement assays. Furthermore, a K<sub>i</sub> prediction assay was performed by comparing the data with that generated by a homogeneous time-resolved fluorescence (HTRF) assay. SNAP-V<sub>2</sub>R@GMF-BG was also used to screen hit compounds from natural products. After SNAP-V<sub>2</sub>R@GMF-BG was incubated with the total extract, the ligand that binds to V<sub>2</sub>R could be separated and subjected to LC–MS analysis for identification. Baicalein was screened from *Clerodendranthus spicatus* and verified as a potential V<sub>2</sub>R antagonist. This V<sub>2</sub>R-immobilized GMF platform can help determine the affinity of V<sub>2</sub>R-binding hit compounds and screen the compounds efficiently and accurately.

**Keywords** Type-2 vasopressin receptor · Hit compound · Target immobilization · Glass microfiber membranes · SNAP-tag · Natural product

## Abbreviations

|                  |  |
|------------------|--|
| AVP              | Arginine vasopressin                                 |
| GPCR             | G protein-coupled receptor                           |
| TR-FRET          | Time-resolved fluorescence resonance energy transfer |
| V <sub>2</sub> R | Type-2 vasopressin receptor                          |
| GMF              | Glass microfiber filters                             |
| BG               | O <sup>6</sup> -Benzylguanine                        |

|      |  |
|------|--|
| CS   | <i>Clerodendranthus spicatus</i>       |
| HTRF | Homogeneous time-resolved fluorescence |

## Introduction

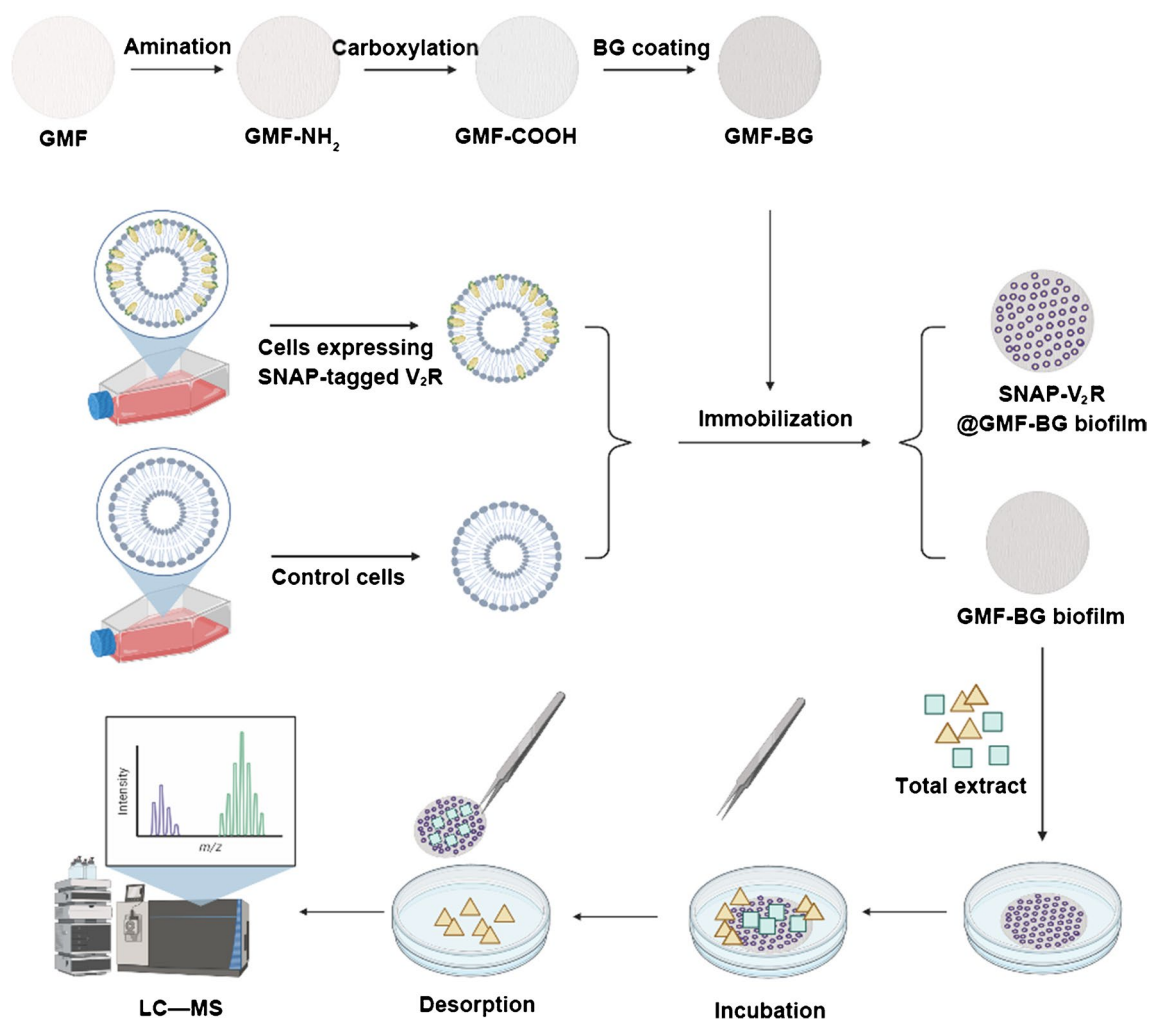
G protein-coupled receptors (GPCRs) are the largest family of cell surface receptors. These receptors can interact with a plethora of signaling molecules and transmit signals from the extracellular side into the intracellular side [1]. GPCRs are primary targets for drug discovery and development. Currently, approximately one-third of FDA-approved drugs target GPCRs to exert their therapeutic effects [2]. Therefore, massive efforts have been dedicated to screening hit compounds with high binding affinities. In addition, traditional assays for affinity determination, such as the homogeneous time-resolved fluorescence (HTRF) assay or radio–ligand binding assay, require a reference compound to be labeled; thus, the methods are labor- and cost-intensive [3, 4].

Yinan Wang and Yan He contributed equally in the making of this manuscript.

✉ Dongzhi Yang  
dongzhiy@xzhmu.edu.cn

✉ Dong Guo  
guo@xzhmu.edu.cn

<sup>1</sup> Jiangsu Key Laboratory of New Drug Research and Clinical Pharmacy, Xuzhou Medical University, 209 Tongshan Road, Xuzhou 221004, Jiangsu, China



**Scheme 1** Scheme of the preparation and application of SNAP-V<sub>2</sub>R@GMF-BG

In the present study, we chose the type-2 vasopressin receptor (V<sub>2</sub>R) as a prototypical GPCR. The receptor is highly expressed in the epithelial cells of the renal collecting duct and the distal tubule [5] and is a validated drug target for autosomal dominant polycystic kidney disease (ADPKD) [6, 7]. Numerous V<sub>2</sub>R antagonists have been developed. In particular, tolvaptan is the first-in-class V<sub>2</sub>R antagonist for the treatment of ADPKD [8]. However, tolvaptan has received a safety warning in the USA and EU because of its potential hepatotoxicity [9]. Hence, it is necessary to discover new V<sub>2</sub>R antagonists for unmet medical needs. Natural products are valuable resources for hit identification. However, to examine the binding affinity of these products, the component of interest must normally be purified from the complex matrices [10]. The traditional procedure for separating and purifying natural products is a lengthy process, which largely hinders the discovery of hit compounds from natural products. Therefore, it is highly desirable to develop a novel method for the affinity determination and

rapid identification of hit compounds that exhibit reasonable binding affinity from complex natural extracts.

Herein, we applied a label-free binding assay to identify hit compounds for the V<sub>2</sub>R and determine their binding affinity. The V<sub>2</sub>R receptor is engineered with a SNAP-tag, which is a modified form of the human O<sup>6</sup>-alkylguanine-DNA alkyltransferase [11, 12], while the glass microfiber (GMF) membranes were coated with O<sup>6</sup>-benzylguanine (BG). The SNAP-tag can undergo a self-labeling reaction to form a covalent bond with O<sup>6</sup>-benzylguanine (BG) derivatives. As a result, we modified BG on the surface of carboxylated GMF and captured SNAP-tagged V<sub>2</sub>R from the cell membrane, establishing a SNAP-V<sub>2</sub>R@GMF-BG screening platform. After the V<sub>2</sub>R-immobilized GMF membranes are incubated with the total extract, the ligand that binds to V<sub>2</sub>R can be physically separated and subjected to LC-MS analysis for compound identification [13, 14] (Scheme 1). With this assay, we first tested a series of known V<sub>2</sub>R antagonists followed by HPLC to obtain their K<sub>i</sub> values and compared them

to the data tested by performing a HTRF. After assay validation, we used this assay to identify hit compounds from the total extract of *Clerodendranthus spicatus* (CS). Baicalin was identified as a promising hit compound for V<sub>2</sub>R. This GPCR-immobilized GMF platform could promote the affinity determination and discovery of hit compounds from complex systems.

## Material and methods

### Materials and reagents

GMF membranes (grade GF/C) were purchased from Whatman (GE Healthcare Life Sciences, USA). CHO cells stably expressing high V<sub>2</sub>R (CHO<sub>h</sub>V<sub>2</sub>R) were produced by Jiangsu Laisen Institute of Biotechnology Co, Ltd. (Zhenjiang, China). Stable SNAP-tagged human V<sub>2</sub>R HEK293 cells were purchased from Cisbio Bioassays (Shanghai, China). Dulbecco's modified Eagle's medium (DMEM) and Roswell Park Memorial Institute (RPMI) 1640 medium were purchased from Thermo Fisher Co, Ltd. (Shanghai, China), and newborn calf serum was purchased from Gibco Co, Ltd. (Shanghai, China).

Tolvaptan, conivaptan, lixivaptan, vasopressin, pioglitazone, and T62 were produced by MedChemexpress Co., Ltd. (USA). Other V<sub>2</sub>R ligands were previously synthesized in our laboratory. *Clerodendranthus spicatus* (Lot: 210603) was purchased from the GuoDa drugstore (Shanghai, China). All other chemicals were purchased from standard commercial sources.

### Cell culture and preparation of cell membranes

The SNAP-tagged V<sub>2</sub>R cell culture was maintained in DMEM mixed with 10% newborn calf serum, 100 IU/mL penicillin, 100 µg/mL streptomycin, and 0.6 mg/mL neomycin at 37 °C in a 5% CO<sub>2</sub> incubator [15]. The CHO hV<sub>2</sub>R cell line was maintained in RPMI 1640 medium mixed with 10% newborn calf serum, 100 IU/mL penicillin, 100 µg/mL streptomycin, and 3 µg/mL puromycin at 37 °C in a 7% CO<sub>2</sub> incubator.

The SNAP-tagged V<sub>2</sub>R cells were collected by a cell scraper and washed with PBS three times. Tris-HCl (50 mM, pH 7.4) was added to the cell pellet, dispersed by a homogenizer (T25, IKA Co., German), and then ruptured by an ultrasonic cell disruptor (JY92-IIDN, Ningbo Scientz Biotechnology Co., Ltd, China). Subsequently, the mixture was centrifuged at 1000×g for 10 min at 4 °C to collect the supernatant. Finally, the supernatant was centrifuged at 14,000×g for 30 min to obtain the SNAP-V<sub>2</sub>R cell membranes. The protein concentration of the obtained cell membranes was quantified by using a BCA kit. In addition,

wild-type HEK293 cells were treated by the same experimental procedure and used as control samples.

### Preparation of SNAP-V<sub>2</sub>R@GMF-BG

GMF was cut into 6-mm-diameter discs and washed with NaOH (1 M) for 2 h and HCl (2 M) for another 2 h. GMF pieces were then immersed in 95% alcohol for 10 min and transferred to an oven for drying at 45 °C for 2 h.

To coat the GMFs, 20 pieces of GMF were first added into 10 mL of Tris-HCl (10 mM, pH 8.5) mixed with dopamine (DA) and polyethylene imine (PEI), and the mixture was placed on a shaker at 100 r/min for 10 h. After the reaction, the dopamine-modified GMF (GMF-DA) was obtained and pulled out by a tweezer and then transferred to an oven at 45°C for 2 h. Second, GMF-DA was added into dichloromethane mixed with triethylamine and succinic anhydride, and the mixture was placed on a shaker at 100 r/min for 48 h. After a dichloromethane wash was performed, the carboxyl-modified GMF (GMF-COOH) was obtained and then transferred to an oven at 45°C for 2 h. Third, appropriate amounts of GMF-COOH, 1-hydroxybenzotriazole (HOBT), and triethylamine were added into dichloromethane and stirred in an ice bath for 30 min. Then, 1-(3-dimethylaminopropyl)-3-ethylcarbodiimide hydrochloride (EDCI) was added for another 10 h of reaction. Finally, BG was added to react for 20 h. After repeated elution with dichloromethane, the BG-bonded GMF (GMF-BG) was obtained and transferred to the oven at 45°C for 2 h before use.

SNAP-V<sub>2</sub>R cell membranes and GMF-BG were mixed in PBS and incubated for 30 min at 4 °C, generating SNAP-V<sub>2</sub>R@GMF-BG. Afterward, the surfaces of SNAP-V<sub>2</sub>R@GMF-BG were rinsed three times with PBS to remove the unreacted substances. In the same procedure, GMF-BG coated with cell membranes from control cells was used as a control platform to evaluate nonspecific binding and stored in a glass bottle at 4 °C before use.

### Characterization of SNAP-V<sub>2</sub>R@GMF-BG

The surface morphology of SNAP-V<sub>2</sub>R@GMF-BG was measured by a scanning electron microscope (SEM, Hitachi, Tokyo, Japan). The chemical properties of the modified GMF were observed by Fourier transform infrared spectrophotometry (FT-IR, IRAffinity-1S, Shimadzu, Japan) and X-ray photoelectron spectroscopy (XPS; ESCALAB 250xi spectrometer, Thermo Fisher, USA).

To further validate the coating efficiency, fluorescent dye DiI staining was used to label the cell membranes of SNAP-tagged V<sub>2</sub>R cells. DiI solution (1 mg/mL, dissolved in DMSO) was added to the cell membrane suspension, and the mixed solution was stored in the dark for 8 h at 4 °C. The mixed solution was centrifuged at 3000×g for 5 min

to collect DiI-labeled cell membranes and washed with PBS to remove excess DiI. The DiI-labeled cell membranes were prepared to generate SNAP-V<sub>2</sub>R@GMF-BG using the same procedure and observed under an inverted fluorescence microscope (IFM, BX43, Olympus, USA). GMF coated with cell membranes was observed with an excitation wavelength of 549 nm and emission wavelength of 565 nm. The DiI-labeled cell membranes should be marked with red fluorescence.

The surface potential of the modified GMF was recorded by a zeta potential analyzer (PSS Nicomp380ZLS, USA) to analyze the chemical state of the surface. Dried GMF or modified GMF was crushed to powder and dispersed in pure water and then placed in a sonic bath for 10 min. The ultrasonic solution was diluted with water and transferred to a clean tube before the potential test.

### Specificity of SNAP-V<sub>2</sub>R@GMF-BG

Firstly, tolvaptan was applied as a positive control to optimize assay condition. Next, tolvaptan, conivaptan, and lixivaptan were applied as the positive control ligands to evaluate the specificity of SNAP-V<sub>2</sub>R@GMF-BG. In addition, the adenosine A1 receptor activator T62 and PPAR $\gamma$  activator pioglitazone were selected as negative controls. Therefore, a mixed solution of tolvaptan, conivaptan, lixivaptan, pioglitazone, and T62 dissolved in methanol/PBS (v/v = 5:95) was prepared, and the concentrations were all 10  $\mu$ mol/L for the five compounds. A piece of SNAP-V<sub>2</sub>R@GMF-BG film and 0.6 mL of mixed solution were coincubated on a shaker at 100 r/min for 30 min, and then the cell membrane-coated GMF was removed by tweezers and washed with 5% acetic acid three times. Next, cell membrane-coated GMF was placed in an EP tube containing 0.6 mL of menthol/PBS (v/v, 1:1) under ultrasonic conditions for 20 min to elute the V<sub>2</sub>R-binding components. Finally, the residual eluent was collected and filtered through a 0.22- $\mu$ m microporous membrane before HPLC analysis.

HPLC was used to quantify the components in the eluent, a column (4.6  $\times$  250 mm, 5  $\mu$ m, Phenomenex) was employed for chromatographic separation, and the column temperature was 35  $^{\circ}$ C. The mobile phase was composed of water and methanol (20/80, v/v) with an isocratic gradient elution program. The flow rate was 1.0 mL/min, and the detection wavelength was 254 nm. Triplicate experiments were performed for all detections.

### Binding experiments with SNAP-V<sub>2</sub>R@GMF-BG

To evaluate the adsorption capacity of SNAP-V<sub>2</sub>R@GMF-BG, static and dynamic adsorption experiments were performed. The adsorption ratio (mg/g) of tolvaptan was used to evaluate adsorption capacity, which was calculated as  $m_a/m_0$ ,

where  $m_a$  (mg) represented the mass of adsorptive and subsequently eluted tolvaptan and  $m_0$  (mg) represented the mass of added tolvaptan for incubation.

For static adsorption tests, a piece of SNAP-V<sub>2</sub>R@GMF-BG film was added to 0.6 mL of tolvaptan solution at different concentrations (0.5, 1.0, 2.0, 5.0, 10, and 15  $\mu$ mol/L, dissolved in methanol/PBS, v/v = 5:95) and then incubated for 20 min. For dynamic adsorption tests, a piece of SNAP-V<sub>2</sub>R@GMF-BG film was added to 0.6 mL of tolvaptan solution (10  $\mu$ mol/L), which was then incubated for 1, 2, 5, 10, 15, 20, and 30 min. After the washing steps, the final eluted tolvaptan was quantitatively analyzed by HPLC.

### Activity evaluation function of SNAP-V<sub>2</sub>R@GMF-BG

In our previous studies, we obtained a series of tolvaptan derivatives with different  $K_i$  values [16], and these derivatives were applied to explore the relation between the adsorption ratio and  $K_i$  values. Detailed chemical information on the 9 tolvaptan derivatives is listed in Fig. 1. The experimental procedure complied with the “Specificity of SNAP-V<sub>2</sub>R@GMF-BG” section.

### Application of SNAP-V<sub>2</sub>R@GMF-BG to discover hit compounds from natural products

Dried CS powder was extracted with 75% ethanol under ultrasonic conditions for 30 min. The extracting solution was centrifuged at 4000 rpm for 3 min, filtered through a 0.22- $\mu$ m membrane filter, diluted with PBS, and then stored at 4  $^{\circ}$ C before use. A piece of SNAP-V<sub>2</sub>R@GMF-BG film was incubated with 1 ml of CS extracted solution for 30 min, and a subsequent ligand screening procedure was performed in the same manner as in the “Specificity of SNAP-V<sub>2</sub>R@GMF-BG” section. Screening based on the control platform was also performed with the extract of CS to eliminate non-specific binding.

After the screening procedure was performed, LC coupled with high-resolution mass spectrometry (HRMS, Orbitrap Exploris 120, Thermo Fisher Scientific, USA) was utilized to analyze and identify compounds targeting V<sub>2</sub>R from the eluate of CS. The detailed LC–MS/MS conditions are presented in the supporting information. By comparing the peak area of identified chemical constituents with that of the control group, the potential V<sub>2</sub>R inhibitors from CS could be screened out.

### HTRF assay

A homogenous time-resolved fluorescence resonance energy transfer (TR-FRET) assay was adopted to determine the  $K_i$  values of hit compounds, and then fluorescence was recorded at 665 and 620 nm using a microplate reader (LUX, Thermo

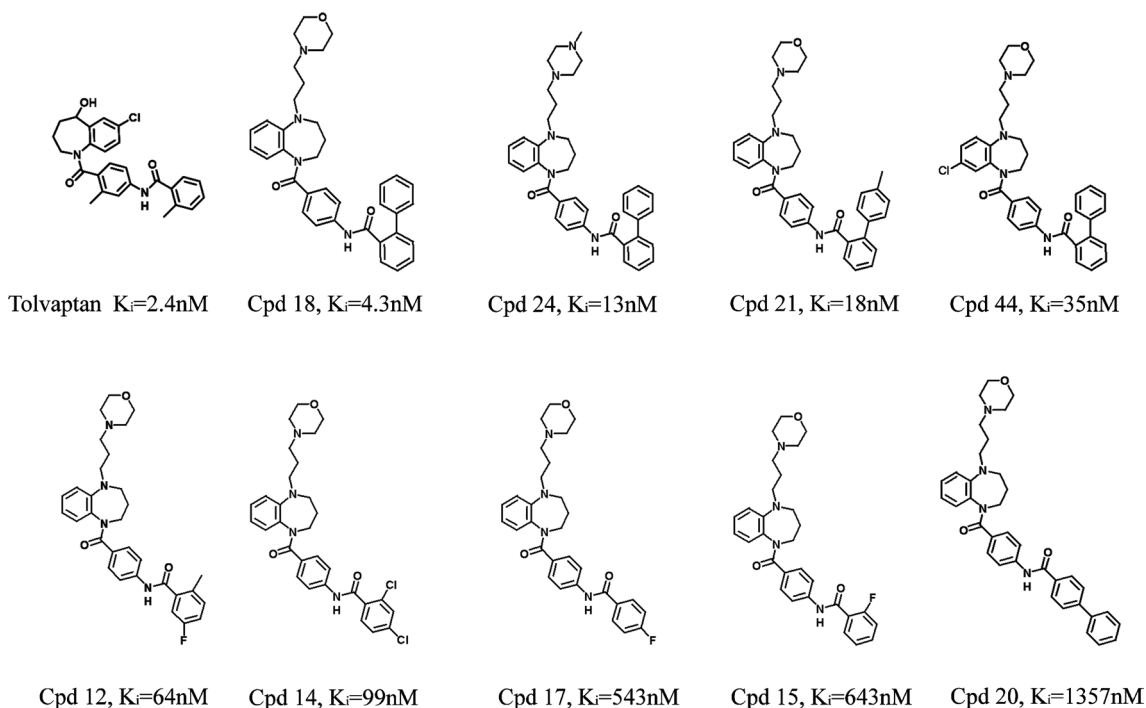


**Fig. 1** The structural formula and  $K_i$  values of tolvaptan and its derivatives [16]

Scientific Varioskan, USA) [14]. For further verification, PyMOL v1.3 software was used to simulate the molecular recognition process and binding energies between  $V_2R$  (PDB ID: 7BB7) and target compounds.

### cAMP assays

$V_2R$  exhibits a stimulatory effect on the enzyme adenylate cyclase. Under an inhibitor, adenosine-3',5'-cyclic monophosphate (cAMP) is downregulated by  $V_2R$ . Therefore, we examined the functional effects of the screened compounds through a cAMP assay. The cAMP level was measured by a cAMP-Gi kit following the manufacturer's instructions (Cisbio Bioassays, Shanghai) as described in our previous study [17]. Briefly, CHO $V_2R$  cells were incubated with the target compounds for 30 min, followed by stimulation with 1 nM vasopressin for 1 h at 37 °C. Then, cells were precipitated, resuspended, and stimulated with vasopressin to accumulate cAMP. Consecutively, cryptate-labeled anticAMP antibody and dye-labeled cAMP were added for 1 h. Signals were recorded at 665 nm and 620 nm by a microplate reader. All data are shown as the mean  $\pm$  SEM of three independent experiments.

## Results

### Characterization of SNAP- $V_2R$ @GMF-BG

Scanning electron microscopy was utilized to visualize the morphology of the GMF surfaces and cell membrane coating areas. Morphological changes in GMF could be clearly observed. The rare GMF was composed of glass fibers with a diameter of approximately 1  $\mu\text{m}$ , which exhibited a clean and smooth surface (Fig. 2A). In comparison, GMF surfaces coated with cell membranes became rougher (Fig. 2B), which indicated that the cell membranes had immobilized on the GMF surface [18].

To further confirm the immobilization of cell membranes on GMF, inverted fluorescence microscope images were obtained. Under the transmitted field, the tight surface of GMF and pyknotic surface of SNAP- $V_2R$ @GMF-BG were observed (Fig. 2C, D). After fluorescence excitation at 549 nm, no red fluorescence was detected at 565 nm in the field of GMF (Fig. 2E), whereas red fluorescence was observed in the SNAP- $V_2R$ @GMF-BG images



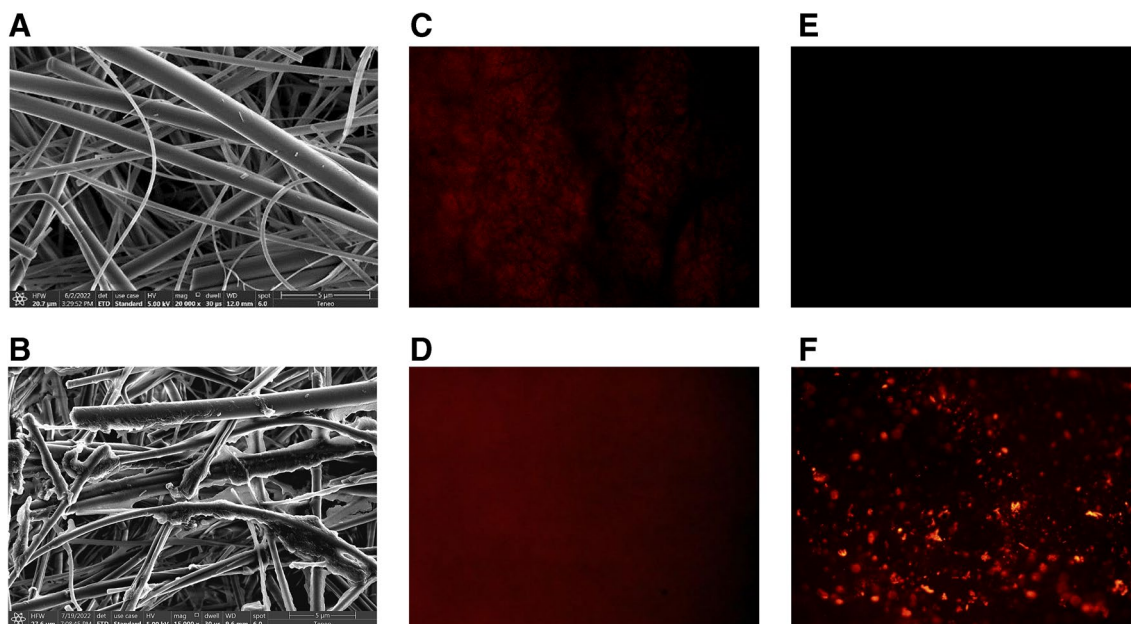


**Fig. 2** Characterization images of GMF and SNAP-V<sub>2</sub>R@GMF-BG. Scanning electron microscopy images of the surface of GMF (A) and SNAP-V<sub>2</sub>R@GMF-BG (B); inverted fluorescence microscopy images of the surface of GMF (C) and SNAP-V<sub>2</sub>R@GMF-BG (D)

with transmitted light; red fluorescence images of the surface of GMF (E) and SNAP-V<sub>2</sub>R@GMF-BG (F) with an excitation wavelength of 549 nm and an emission wavelength of 565 nm

**Fig. 3** Characterization of FT-IR, X-ray photoelectron spectroscopy, and zeta potentials. FT-IR spectra of GMF and GMF-BG (A); XPS wide scans of bare GMF, GMF-BG, and SNAP-V<sub>2</sub>R@GMF-BG (B); and fine spectral scanning of P 2p (C). Zeta potentials of GMF, GMF-BG, and SNAP-V<sub>2</sub>R@GMF-BG (D)

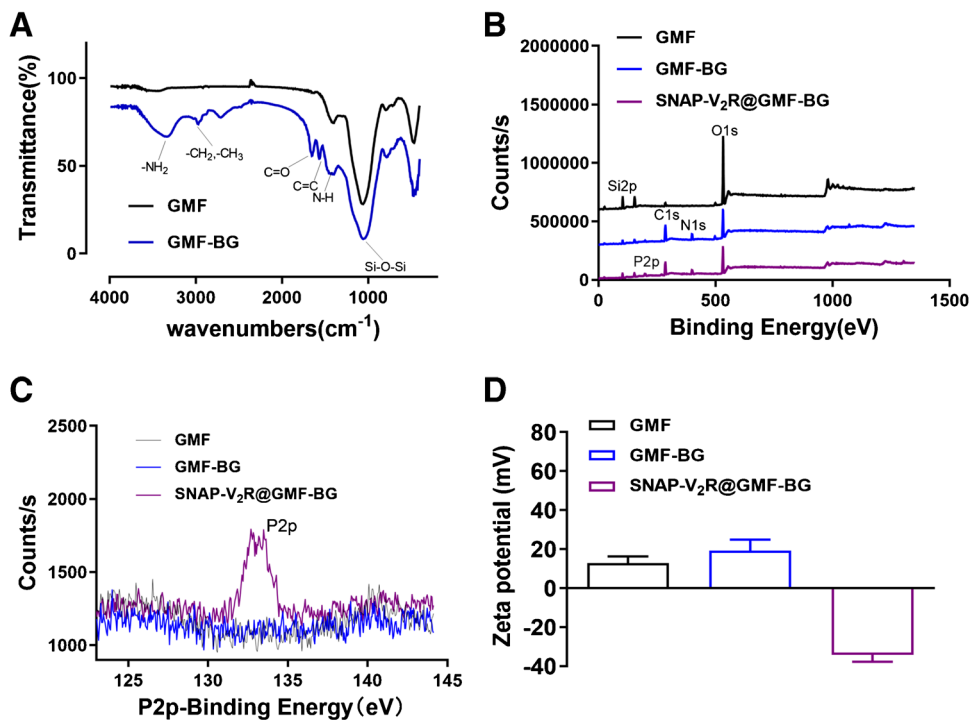


(Fig. 2F), indicating the distribution of DiI-labeled cell membranes on GMF. The results were consistent with the morphological results of scanning electron microscopy, confirming the successful bioimmobilization of cell membranes on the GMF.

As a supplement, FT-IR measurements in the 500–4000  $\text{cm}^{-1}$  range were obtained to characterize BG groups on the GMF (Fig. 3A). The peak at 1020  $\text{cm}^{-1}$  was the absorption peak of the Si–O–Si groups of GMF, which was observed in GMF and GMF-BG [19]. In the FT-IR

spectrum of GMF-BG, the peak at  $1566\text{ cm}^{-1}$  (benzene C–C stretching vibration) and the peak at  $3352\text{ cm}^{-1}$  (amidogen N–H stretching) were attributed to the chemical groups of benzylguanine. In addition, the peak at  $1651\text{ cm}^{-1}$  (C=O stretching vibration) and the peak at  $1486\text{ cm}^{-1}$  (N–H stretching vibration) were attributed to the generation of amido bonds, which was caused by the substitution of BG [20–22]. All the characteristic peaks demonstrated that the BG-modified GMF was successfully prepared.

The availability of functional groups and chemical compositions were further characterized by X-ray photoelectron spectroscopy analysis. The spectrum is shown in Fig. 3B, and the relative content of each element can be found in Table S1. The wide scan of the GMF showed that it was mainly composed of Si and O, and there was no significant peak attributed to N [23]. After bonding with BG, the relative content of N and C in GMF-BG increased, suggesting that BG was successfully modified. However, following coating with cell membranes, the X-ray photoelectron spectroscopy spectrum of SNAP-V<sub>2</sub>R@GMF-BG showed peaks at the P element. The peak of P 2p (Fig. 3C) is a key marker of phospholipids in cell membranes, suggesting that the cell membranes were successfully coated.

The zeta potentials were assayed in pure water, and those of raw GMF and GMF-BG were 12.8 mV and 19.1 mV, respectively (Fig. 3D), which showed the expected transformation of functional groups in GMF. The zeta potential of SNAP-V<sub>2</sub>R@GMF-BG was changed to  $-34.1\text{ mV}$ , indicating that the cell membranes were successfully loaded on the surface of GMF [24].

## Optimizing the experimental conditions

To obtain the best screening efficiency, the operating conditions, including the concentration of cell membranes, type of eluent solvent, elution solvent volume and elution time, were studied [25]. Tolvaptan was applied as a positive control to optimize assay condition.

The amount of cell membrane loaded on the GMF depends upon the concentration of cell membrane. Thus, the effect of cell membrane concentration in a range of 0.07–3.5 mg/mL was investigated. Figure 4A shows that the adsorption ratio of tolvaptan increased with increasing cell membrane concentration, and the highest binding of tolvaptan was obtained at a concentration of 0.35 mg/mL. As the concentration of cell membranes further increased, the tolvaptan amount did not change significantly, indicating that the cell membrane loading had reached saturation. Therefore, the cell membrane concentration was chosen as 0.35 mg/mL.

The elution step was an important process that affected the recovery of tolvaptan. Different kinds of elution solvents, including PBS, 0.1% acetic acid (AA), 0.5% AA and a PBS–methanol mixture (1:1, v/v), were investigated in this study. As shown in Fig. 4B, the PBS–methanol mixture achieved the best elutropic performance and exhibited the largest adsorption ratio of tolvaptan. As a result, the PBS–methanol mixture (1:1, v/v) was selected as the elution solvent. Furthermore, the effect of the elution solvent volume (0.4–5 mL) was investigated (Fig. 4C). The results suggested that 0.6 mL of PBS–methanol mixture (1:1, v/v)

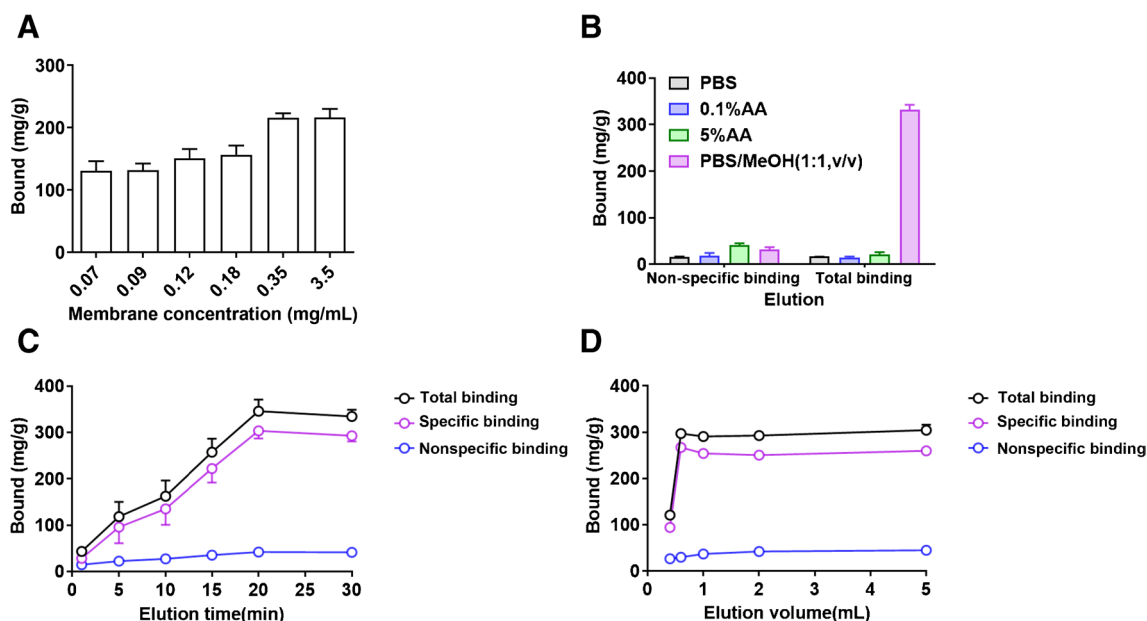


**Fig. 4** Optimization of the experimental procedure. **A** The concentration of cell membranes. **B** Types of different elution solvents. **C** Elution solvent volume. **D** Elution time

was enough to obtain satisfactory recovery, and no change was observed when the volume further increased. In addition, elution times from 1 to 30 min were investigated to obtain the optimal elution time. As illustrated in Fig. 4D, the elution efficiency of tolvaptan reached a maximum at 20 min. Based on the above results, 0.6 mL of PBS–methanol mixture and 20 min of elution time were chosen for the subsequent experiments.

### Specificity of SNAP-V<sub>2</sub>R@GMF-BG

The adsorption ratios of tolvaptan (positive control) and T62 (negative control) using rare GMF and V<sub>2</sub>R@GMF-COOH (nonspecific immobilization, i.e., cell membranes were immobilized on GMF-COOH by condensation of amino and carboxyl groups) were measured and compared. As shown in Fig. 5A, the SNAP-V<sub>2</sub>R@GMF-BG platform had the largest adsorption ratio of tolvaptan and much larger than that of T62, indicating that the target immobilization exhibited excellent specificity.

The dynamic binding of SNAP-V<sub>2</sub>R@GMF-BG with different incubation times of tolvaptan was investigated. As presented in Fig. 5B, as time increased, the specific binding capacity of tolvaptan for SNAP-V<sub>2</sub>R@GMF-BG increased slowly before 20 min and reached equilibrium at a 30 min concentration.

We also tried the mixture to mimic the complexity of natural product. The chromatogram of the mixture of tolvaptan and T62 is shown in Fig. 5C-1. After

the screening procedure, only tolvaptan was eluted from SNAP-V<sub>2</sub>R@GMF-BG and detected in the chromatogram (Fig. 5C-2), which indicated that SNAP-V<sub>2</sub>R@GMF-BG could selectively recognize tolvaptan due to its specific affinity for V<sub>2</sub>R. The binding components eluted from SNAP-V<sub>2</sub>R@GMF-BG were named total binding. To further verify the specificity, the control platform was also used to exhibit a nonspecific binding chromatogram, and trace amounts of both tolvaptan and T62 were detected in the eluent (Fig. 5C-3). Then, the nonspecific binding was subtracted from the total binding to get the specific binding. These final specific binding results (Fig. 5C-4) demonstrated that SNAP-V<sub>2</sub>R@GMF-BG could be used to selectively screen active ligands from a mixture.

The adsorption ratios of tolvaptan, conivaptan, lixivaptan, pioglitazone, and T62 by SNAP-V<sub>2</sub>R@GMF-BG are shown in Fig. 5D. Tolvaptan, conivaptan, and lixivaptan were detected by SNAP-V<sub>2</sub>R@GMF-BG. In contrast, pioglitazone and T62 showed almost no signals, indicating the excellent specificity of SNAP-V<sub>2</sub>R@GMF-BG. In addition, the affinity of pioglitazone/T62 binding to the V<sub>2</sub>R was tested by HTRF (Fig. S1), which demonstrated that pioglitazone and T62 were negative ligands for V<sub>2</sub>R.

### Correlation between the adsorption ratio and $K_i$ of ligand compounds by SNAP-V<sub>2</sub>R@GMF-BG

Under the optimized conditions of SNAP-V<sub>2</sub>R@GMF-BG, the correlation between the adsorption ratio and  $K_i$  of the 10

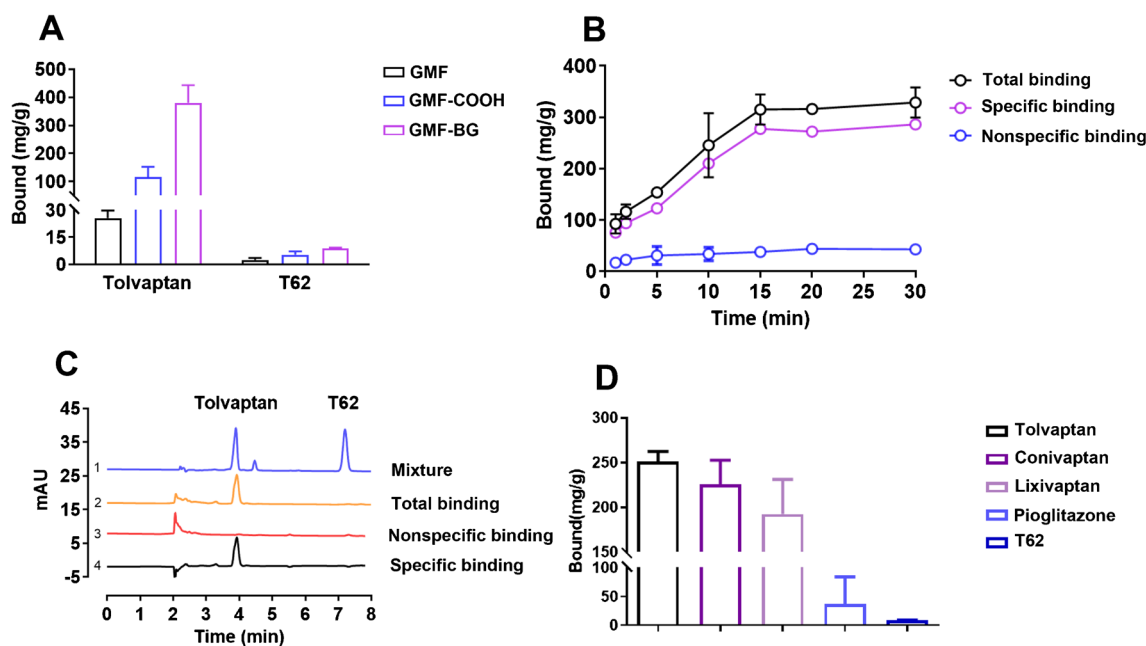


**Fig. 5** Adsorption ratio of tolvaptan and T62 by different platforms (A); dynamic adsorption curves of SNAP-V<sub>2</sub>R@GMF-BG (B); chromatogram of the mixture of tolvaptan and T62 (C-1); chromatogram of the specific binding of tolvaptan and T62 (C-4); adsorption ratio of

tolvaptan, conivaptan, lixivaptan, pioglitazone, and T62 (D)



ligand compounds listed in Fig. 1 was investigated. The  $K_i$  values of 10 ligand compounds were measured by HTRF. By plotting the adsorption ratio (mg/g) against  $\log K_i$  (nM), a linear regression plot was obtained, which is illustrated in Fig. 6. The linear equation was  $y = -51.16x + 275.5$ , and the correlation coefficient ( $r$ ) of the fitting curve was 0.996. The results indicated that the  $K_i$  of ligands could be calculated by the adsorption ratio measured by the SNAP- $V_2R$ @GMF-BG platform instead of the traditional experimental determination of  $K_i$ .

### $K_i$ prediction of different types of $V_2R$ ligands using the SNAP- $V_2R$ @GMF-BG platform

To verify the ability of SNAP- $V_2R$ @GMF-BG to predict  $K_i$ ,  $V_2R$  agonists (MCF57 and WAY-151932),  $V_2R$  antagonists (conivaptan and lixivaptan), and benzimidazole  $V_2R$  antagonists (P15, P18, P55, and P80, synthesized in house) were selected as typical test compounds. The detailed chemical information of the above compounds is shown

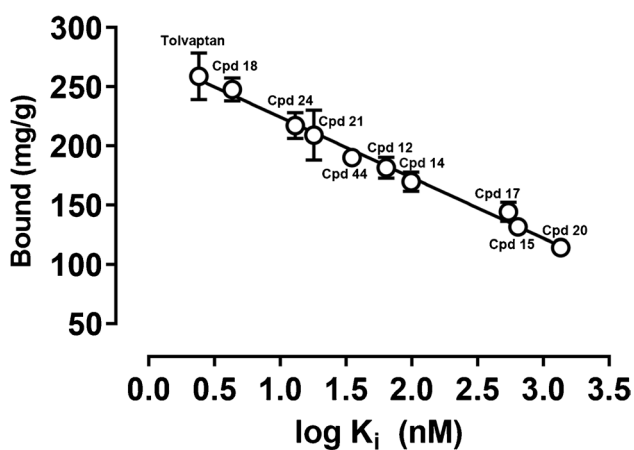


**Fig. 6** The correlation of the adsorption ratio (mg/g) against  $\log K_i$  (nM) based on the SNAP- $V_2R$ @GMF-BG platform

**Table 1**  $K_i$  predictive ability of SNAP- $V_2R$ @GMF-BG for  $V_2R$  ligands

| Type of compounds        | Compound name | Adsorption ratio (mg/g) | $K_i$ (nM)             |                |
|--------------------------|---------------|-------------------------|------------------------|----------------|
|                          |               |                         | Calculated by equation | HTRF assay     |
| Agonist for $V_2R$       | MCF57         | $137.46 \pm 7.9$        | $448 \pm 25$           | $537 \pm 60$   |
|                          | WAY-151932    | $154.08 \pm 4.0$        | $215 \pm 5.6$          | $394 \pm 21$   |
| Antagonist for $V_2R$    | Conivaptan    | $239.58 \pm 20$         | $7.7 \pm 1.8$          | $2.6 \pm 0.3$  |
|                          | Lixivaptan    | $229.38 \pm 20$         | $14 \pm 2.7$           | $3.1 \pm 0.4$  |
| Benzimidazole antagonist | P15           | $153.43 \pm 5.8$        | $221 \pm 19$           | $294 \pm 59$   |
|                          | P18           | $109.51 \pm 14$         | $1535 \pm 190$         | $1023 \pm 330$ |
|                          | P55           | $162.47 \pm 14$         | $148 \pm 28$           | $60 \pm 32$    |
|                          | P80           | $216.15 \pm 25$         | $17 \pm 1.9$           | $13 \pm 1$     |

in Fig. S2. The experimental procedure complied with the “Specificity of SNAP- $V_2R$ @GMF-BG” section, and three parallel experiments were performed. The adsorption ratio was determined by HPLC, and the  $K_i$  value was calculated according to the equation  $y = -51.16x + 275.5$ . All results are shown in Table 1.  $K_i$  values calculated from the equation were within the same order of magnitude as those measured by the HTRF method. This indicates that SNAP- $V_2R$ @GMF-BG exhibited different adsorption capacities for  $V_2R$  ligands with different  $K_i$  values, and the results also demonstrated the good applicability of the curve for  $V_2R$  ligands.

### Application of SNAP- $V_2R$ @GMF-BG to discover hit compounds in natural products

We also tried to screen hit compounds from the natural product. After being optimized and validated, the prepared SNAP- $V_2R$ @GMF-BG platform was applied to screen hit compounds of  $V_2R$  inhibitors from CS. The eluent of CS obtained from SNAP- $V_2R$ @GMF-BG was analyzed by HPLC-HRMS for identification under positive and negative ion modes. The chromatograms of extraction of CS, the eluent obtained from SNAP- $V_2R$ @GMF-BG (total binding), and the eluent obtained from the control group (nonspecific binding) are displayed in Fig. 7. Compared with chromatograms of the extract of CS, active compounds were retained after screening by SNAP- $V_2R$ @GMF-BG, and nonspecific binding compounds were then diminished or disappeared after screening by the control platform. The retained peaks of total binding and simultaneously diminished peaks of nonspecific binding represented hit compounds in CS.

After the chromatograms showing total binding and nonspecific binding were analyzed, one significant component peak was confirmed, which should be a ligand recognized from the extraction of CS. After the mass spectrum was analyzed and the results were compared with a self-built database of standard substances (containing approximately 4000 kinds of compounds from natural herbs), baicalein

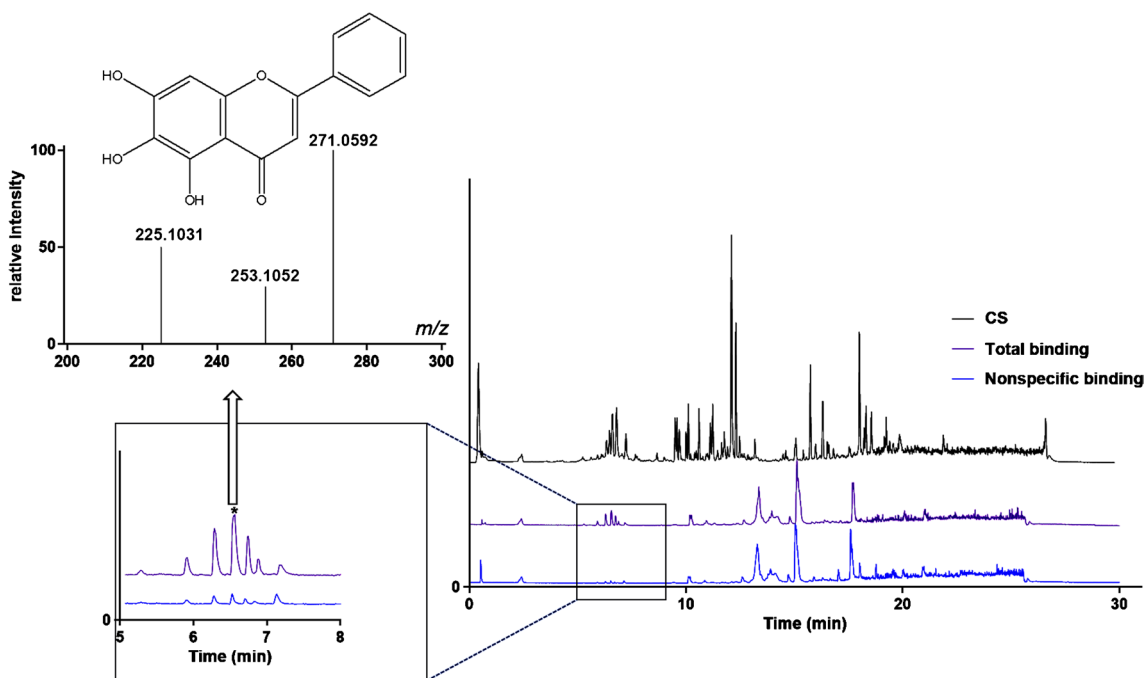


**Fig. 7** TIC chromatograms obtained by LC-HRMS in positive ion mode. TIC chromatogram of initial CS extract (CS); the eluent of CS incubated with SNAP-V<sub>2</sub>R@GMF-BG (total binding); the eluent of CS incubated with the control platform (nonspecific binding)

was identified in the final eluate compared with the control model.

To further confirm the accuracy of the above screening results, the reference substance baicalein was screened using the SNAP-V<sub>2</sub>R@GMF-BG platform, and the results are presented in Fig. 8A. The baicalein peak was present in the chromatogram by HPLC, which further confirmed the accuracy of the SNAP-V<sub>2</sub>R@GMF-BG platform.

### Affinity and pharmacological effects of the targeted components

To verify the binding activity with V<sub>2</sub>R, the  $K_i$  value of baicalein was calculated as 131.2  $\mu$ M by HTRF assay. Interestingly, the adsorption ratio of baicalein was tested as 35 mg/g, and the corresponding  $K_i$  value was calculated as 177.83  $\mu$ M using the equation in the “Correlation between the adsorption ratio and  $K_i$  of ligand compounds by SNAP-V<sub>2</sub>R@GMF-BG” section. The results verified the prediction generated by SNAP-V<sub>2</sub>R@GMF-BG.

A cAMP assay was also utilized to investigate the inhibitory effects of screened components from CS. As shown in Fig. 8B, baicalein inhibited vasopressin-induced cAMP production, and the  $IC_{50}$  value was calculated as 123.4  $\mu$ M. The effects of baicalein and tolvaptan on the basal cAMP level (tested at 100-fold their respective  $K_i$  values and without vasopressin stimulation) were also tested, and they all reduced the basal cAMP level (Fig. 8C). The results showed

that baicalein can specifically target V<sub>2</sub>R and inhibit cAMP and could be utilized as a candidate V<sub>2</sub>R inhibitor for further research. Therefore, the results confirmed that SNAP-V<sub>2</sub>R@GMF-BG could be applied to effectively screen and evaluate potential inhibitors targeting V<sub>2</sub>R from natural products.

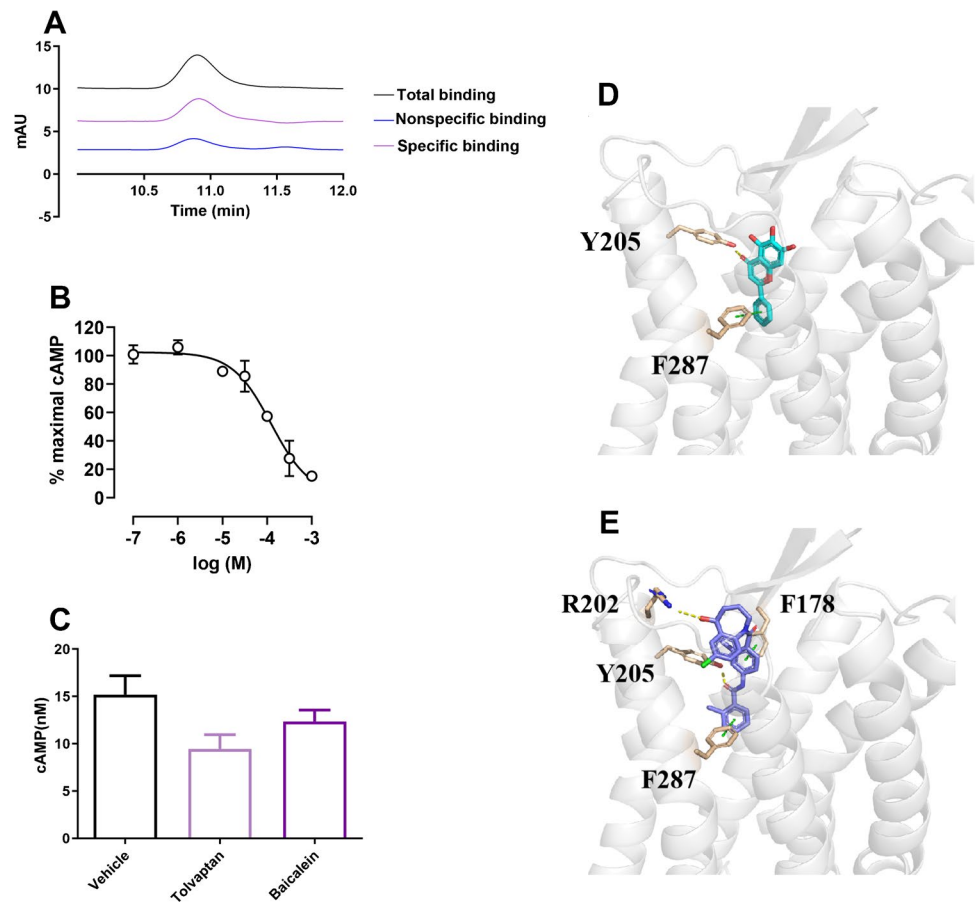
### Molecular docking analysis

The binding modes of the target compounds with V<sub>2</sub>R (PDB ID: 7DW9) were analyzed by molecular docking. Baicalein matched the active pocket of V<sub>2</sub>R well, as shown in Fig. 8D and E. Specifically, Fig. 8D shows the interactions of baicalein with V<sub>2</sub>R through hydrogen bonds and  $\pi$ - $\pi$  stacking with Y205 and F287, showing a binding energy of  $-7.2$  kcal/mol, a result close to that of tolvaptan ( $-7.8$  kcal/mol, Fig. 8E). The docking results indicated that baicalein might potentially be a V<sub>2</sub>R inhibitor.

### Discussion

In the present study, we used crude cell membranes of SNAP-tagged V<sub>2</sub>R cells rather than solubilized and purified V<sub>2</sub>R proteins. First, the V<sub>2</sub>R is inherently instable when extracted from the naive environment in the plasma membrane. Second, the crude membrane still retains the complete biological structure of membrane proteins and enables efficient ligand-receptor interaction. This has been successfully

**Fig. 8** The affinity verification of baicalein for V<sub>2</sub>R. Screening experiment of baicalein by SNAP-V<sub>2</sub>R@GMF-BG (A); concentration-dependent inhibition of cellular cAMP levels by baicalein (B); inhibitory effects of baicalein and tolvaptan on the basal cAMP level (C); molecular docking analysis of V<sub>2</sub>R and potential compounds of baicalein (D) and tolvaptan (E)



applied for the D<sub>2</sub> receptor [26]. Next, we immobilized cell membranes on GMF membranes for compound screening. Doing so enabled physically separating potential V<sub>2</sub>R hit compounds from the total extract of the natural product, and the identified hit compounds could be subsequently collected and subjected to LC–MS analysis for identification. In comparison, previous strategies generally involve physical absorbing the proteins on the magnetic nanoparticle surfaces, which resulted in unstable platforms; this is because the magnetic nanoparticles exhibit self-aggregation properties, and external magnets are needed to recover active components in a solution system [27]. Moreover, the cell membranes easily detached from the nanoparticles, which limited their application and reproducibility.

GMFs are polar hydrophilic membranes with great potential because they are chemically, thermally, and mechanically stable, pH resistant, inexpensive, and convenient to obtain [28, 29]. As a supporting substrate, GMF possesses pore canals and offers many advantages over filter paper [30, 31], which can allow cell insertion; in addition, GMF has been utilized as a robust supporting matrix in many applications [32]. When applied in concert with other functional groups, the GMF surface provided proper support by adhering to the cell membrane and forming a biocompatible polymer

[33]. In this study, V<sub>2</sub>R was targeted immobilized on GMF, and chemical bonding of V<sub>2</sub>R to the surface of GMF can improve the stability, efficiency, and convenience of biomimetic platforms. Owing to the reduction in the nonspecific absorption of cell membranes, this SNAP-V<sub>2</sub>R@GMF-BG platform showed reasonable specificity and stability.

Affinity determination methods, such as the surface plasmon resonance (SPR), HTRF assay, or radio–ligand binding assay, are both labor- and cost-intensive which need special reagents or laboratory conditions. The SNAP-V<sub>2</sub>R@GMF-BG platform supplied a label-free binding strategy, helping to determine the affinity between V<sub>2</sub>R and ligands at low cost. In this study, the  $K_i$  of ligands (baicalein, V<sub>2</sub>R agonists, and antagonists) could be calculated by the adsorption ratio measured by the SNAP-V<sub>2</sub>R@GMF-BG platform, and  $K_i$  values calculated from the equation were close to those measured by the HTRF method. Therefore, SNAP-V<sub>2</sub>R@GMF-BG was verified owing to its  $K_i$  predictive ability.

Hit compounds discovered in natural products have received increasing attention, but there many challenges remain in the screening of active GPCR-targeting ligands from complex matrices [34]. CS is traditionally consumed as a functional beverage for the treatment of renal disease and is known as “kidney tea” in traditional Chinese medicine

[35]. The main active components of CS include flavonoids, terpenoids, lignans, and phenolic acids, which exhibit anti-inflammatory, antioxidant, antiobesity, and diuretic activities [36]. V<sub>2</sub>R ligands are usually discovered as diuretic compounds, so CS was selected to screen hit compounds of V<sub>2</sub>R antagonists given its pharmaceutical effects. In our study several components were screened out from *Clerodendranthus spicatus* by using SNAP-V<sub>2</sub>R@GMF-BG. These included baicalin, which displayed a potent binding affinity for the V<sub>2</sub>R and inhibited cAMP levels. Although baicalin is a main active substance of *Scutellaria baicalensis* Georgi, it is not commonly used for treatment of renal diseases. Thus, we did not select it as our experimental sample in the beginning of the study. We believe baicalin could be screened out as well, provided *Scutellaria baicalensis* Georgi is used. Therefore, the SNAP-V<sub>2</sub>R@GMF-BG platform for screening hit compounds from natural extracts can act as an important supplement to traditional methods.

## Conclusions

In this work, GMF was applied as a carrier for covalent immobilization of cell membranes for the first time, and a novel, inexpensive, simple, and convenient biofilm platform for screening hit compounds was developed by cell membrane-coated GMF. The prepared SNAP-V<sub>2</sub>R@GMF-BG exhibited reasonable specificity and reproducibility and was successfully applied to predict the affinity of V<sub>2</sub>R-targeted hit compounds and selectively screen the compounds from natural products. Finally, baicalin was screened from CS. The developed platform can recognize active ligands for specific receptors from a complex matrix and is a powerful tool for screening and evaluating hit compounds.

**Supplementary Information** The online version contains supplementary material available at <https://doi.org/10.1007/s00216-023-04951-w>.

**Acknowledgements** The authors thank Biotree Biomedical Technology Co., Ltd., for technical assistance with HRMS analysis.

**Author contribution** Yinan Wang: original draft. Yan He: data curation. Xiaojiao Ye: editing and visualization. Yixiao Zhang: methodology. Xiuxiu Huang: validation. Hongli Liu: software. Wenqing Dong: visualization. Dongzhi Yang: supervision. Dong Guo: writing — review and editing.

**Funding** This project was financially supported by the National Natural Science Foundation of China (22077110, 22377103, 8234869), the Natural Science Foundation of Jiangsu Province (BK20200106), the Natural Science Foundation of the Jiangsu Higher Education Institutions of China (20KJA350001, 21KJB350025), and the project of scientific and technological development of traditional Chinese medicine in Jiangsu province (MS2021106). This project was partly performed at the National Demonstration Center for Experimental Basic Medical Science Education (Xuzhou Medical University) and funded by the

Innovation and Entrepreneurship Training Program for College Students in Jiangsu Province (grant number 202210313024Z).

## Declarations

**Conflict of interest** The authors declare no competing interests.

## References

- Maryanoff BE. Adventures in drug discovery: potent agents based on ligands for cell-surface receptors. *Acc Chem Res.* 2006;39(11):831–40. <https://doi.org/10.1021/ar040112l>.
- Hauser AS, Attwood MM, Rask-Andersen M, Schiöth HB, Gloriam DE. Trends in GPCR drug discovery: new agents, targets and indications. *Nat Rev Drug Discov.* 2017;16(12):829–42. <https://doi.org/10.1038/nrd.2017.178>.
- Rebeck R, Ginsburg KS, Ko CY, Fasoli A, Rusch K, Cai GF, Dong X, Thomas DD, Bers DM, Cornea RL. Synergistic FRET assays for drug discovery targeting RyR2 channels. *J Mol Cell Cardiol.* 2022;168:13–23. <https://doi.org/10.1016/j.yjmcc.2022.04.002>.
- Wang D, Zhao W, Zhang Z, Zhang Y, Li J, Huang W. Design, synthesis and biological evaluation of novel biphenylsulfonamide derivatives as selective AT(2) receptor antagonists. *Front Chem Chin.* 2022;10:984717. <https://doi.org/10.3389/fchem.2022.984717>.
- Fenton RA, Brond L, Nielsen S, Praetorius J. Cellular and subcellular distribution of the type-2 vasopressin receptor in the kidney. *Am J Physiol Renal Physiol.* 2007;293(3):F748–760. <https://doi.org/10.1152/ajprenal.00316.2006>.
- Corneec-Le Gall E, Alam A, Perrone RD. Autosomal dominant polycystic kidney disease. *Lancet.* 2019;393(10174):919–35. [https://doi.org/10.1016/s0140-6736\(18\)32782-x](https://doi.org/10.1016/s0140-6736(18)32782-x).
- Zhang H, Yan W, Sun Y, Yuan H, Su L, Cao X, Wang P, Xu Z, Hu Y, Wang Z, Wang Y, Fu K, Sun Y, Chen Y, Cheng J, Guo D. Long residence time at the vasopressin V2 receptor translates into superior inhibitory effects in ex vivo and in vivo models of autosomal dominant polycystic kidney disease. *J Med Chem.* 2022;65(11):7717–28. <https://doi.org/10.1021/acs.jmedchem.2c00011>.
- Yamamura YNS, Itoh S, Hirano T, Onogawa T, Yamashita T, Yamada Y, Tsujimae K, Aoyama M, Kotosai K, Ogawa H, Yamashita H, Kondo K, Tominaga M, Tsujimoto G, Mori T. OPC-41061, a highly potent human vasopressin V2-receptor antagonist: pharmacological profile and aquaretic effect by single and multiple oral dosing in rats. *J Pharmacol Exp Ther.* 1998;287:860–7.
- FDA Drug Safety Communication: FDA warns of serious liver injury risk with hepatitis C treatments Viekira Pak and Technivie. Drug Safety Communication. 2015. <https://www.drugs.com/fda/hepatitis-c-treatments-viekira-pak-technivie-safety-communication-risk-serious-liver-injury-13781.html>. Accessed 22 Oct 2015.
- Shar PA, Tao W, Gao S, Huang C, Li B, Zhang W, Shahen M, Zheng C, Bai Y, Wang Y. Pred-binding: large-scale protein-ligand binding affinity prediction. *J Enzyme Inhib Med Chem.* 2016;31(6):1443–50. <https://doi.org/10.3109/14756366.2016.1144594>.
- Keppeler A, Gendreizig S, Gronemeyer T, Pick H, Vogel H, Johnsson K. A general method for the covalent labeling of fusion proteins with small molecules in vivo. *Nat Biotechnol.* 2003;21(1):86–9. <https://doi.org/10.1038/nbt765>.
- Chidley C, Haruki H, Pedersen MG, Muller E, Johnsson K. A yeast-based screen reveals that sulfasalazine inhibits



- tetrahydrobiopterin biosynthesis. *Nat Chem Biol.* 2011;7(6):375–83. <https://doi.org/10.1038/nchembio.557>.
13. Fu J, Jia Q, Liang P, Wang S, Zhou H, Zhang L, Gao C, Wang H, Lv Y, Han S. Targeting and covalently immobilizing the EGFR through SNAP-Tag technology for screening drug leads. *Anal Chem.* 2021;93(34):11719–28. <https://doi.org/10.1021/acs.analchem.1c01664>.
  14. Xu L, Tang C, Li X, Li X, Yang H, Mao R, He J, Li W, Liu J, Li Y, Shi S, Xiao X, Wang X. Ligand fishing with cellular membrane-coated cellulose filter paper: a new method for screening of potential active compounds from natural products. *Anal Bioanal Chem.* 2019;411(10):1989–2000. <https://doi.org/10.1007/s00216-019-01662-z>.
  15. Liu C, Xia L, Fu K, Cao X, Yan W, Cheng J, Roux T, Peletier LA, Yin X, Guo D. Revisit ligand-receptor interaction at the human vasopressin V2 receptor: a kinetic perspective. *Eur J Pharmacol.* 2020;880:173157. <https://doi.org/10.1016/j.ejphar.2020.173157>.
  16. Cao X, Wang P, Yuan H, Zhang H, He Y, Fu K, Fang Q, Liu H, Su L, Yin L, Xu P, Xie Y, Xiong X, Wang J, Zhu X, Guo D. Benzodiazepine derivatives as potent vasopressin V2 receptor antagonists for the treatment of autosomal dominant kidney disease. *J Med Chem.* 2022;65(13):9295–311. <https://doi.org/10.1021/acs.jmedchem.2c00567>.
  17. Yun Y, Chen J, Liu R, Chen W, Liu C, Wang R, Hou Z, Yu Z, Sun Y, IJ AP, Heitman LH, Yin X, Guo D. Long residence time adenosine A1 receptor agonists produce sustained wash-resistant antilipolytic effect in rat adipocytes. *Biochem Pharmacol.* 2019;164:45–52. <https://doi.org/10.1016/j.bcp.2019.03.032>.
  18. Li JL, Gao YH, Jin CX, Wang Y, He M, Dong WW, Zhao J, Li D, Shang HB. Facile surface modification of glass-fiber membrane with silylating reagent through chemical bonding for the selective separation and recycling of diverse dyes from aqueous solutions. *ChemistrySelect.* 2018;3(45):12734–41. <https://doi.org/10.1002/slct.201802943>.
  19. Mhatre AM, Chappa S, Ojha S, Pandey AK. Functionalized glass fiber membrane for extraction of iodine species. *Sep Sci Technol.* 2018;54(9):1469–77. <https://doi.org/10.1080/01496395.2018.1520729>.
  20. Liu J, Zhang HX, Shi YP. Lipase immobilization on magnetic cellulose microspheres for rapid screening inhibitors from traditional herbal medicines. *Talanta.* 2021;231:122374. <https://doi.org/10.1016/j.talanta.2021.122374>.
  21. Phiri I, Eum KY, Kim JW, Choi WS, Kim SH, Ko JM, Jung H. Simultaneous complementary oil-water separation and water desalination using functionalized woven glass fiber membranes. *J Ind Eng Chem.* 2019;73:78–86. <https://doi.org/10.1016/j.jiec.2018.12.049>.
  22. Zhou H, Fu J, Jia Q, Wang S, Liang P, Wang Y, Lv Y, Han S. Magnetic nanoparticles covalently immobilizing epidermal growth factor receptor by SNAP-Tag protein as a platform for drug discovery. *Talanta.* 2022;240:123204. <https://doi.org/10.1016/j.talanta.2021.123204>.
  23. Bandara PC, Nadres ET, Rodrigues DF. Use of response surface methodology to develop and optimize the composition of a chitosan-polyethyleneimine-graphene oxide nanocomposite membrane coating to more effectively remove Cr(VI) and Cu(II) from water. *ACS Appl Mater Interfaces.* 2019;11(19):17784–95. <https://doi.org/10.1021/acsami.9b03601>.
  24. Hu Q, Zhang X, Jia L, Zhen X, Pan X, Xie X, Wang S. Engineering biomimetic graphene nanodecoys camouflaged with the EGFR/HEK293 cell membrane for targeted capture of drug leads. *J Biomater Sci, Polym Ed.* 2020;8(20):5690–7. <https://doi.org/10.1039/d0bm00841a>.
  25. Hu Q, Bu Y, Zhen X, Xu K, Ke R, Xie X, Wang S. Magnetic carbon nanotubes camouflaged with cell membrane as a drug discovery platform for selective extraction of bioactive compounds from natural products. *Chem Eng J.* 2019;364:269–79. <https://doi.org/10.1016/j.cej.2019.01.171>.
  26. Sykes DA, Moore H, Stott L, Holliday N, Javitch JA, Lane JR, Charlton SJ. Extrapyramidal side effects of antipsychotics are linked to their association kinetics at dopamine D2 receptors. *Nat Commun.* 2017;8(1):763. <https://doi.org/10.1038/s41467-017-00716-z>.
  27. Bu Y, Hu Q, Ke R, Sui Y, Xie X, Wang S. Cell membrane camouflaged magnetic nanoparticles as a biomimetic drug discovery platform. *Chem Commun (Camb).* 2018;54(95):13427–30. <https://doi.org/10.1039/c8cc08530g>.
  28. Bandara GC, Heist CA, Remcho VT. Patterned polycaprolactone-filled glass microfiber microfluidic devices for total protein content analysis. *Talanta.* 2018;176:589–94. <https://doi.org/10.1016/j.talanta.2017.08.031>.
  29. Woo S, Park HR, Park J, Yi J, Hwang W. Robust and continuous oil/water separation with superhydrophobic glass microfiber membrane by vertical polymerization under harsh conditions. *Sci Rep.* 2020;10(1):21413. <https://doi.org/10.1038/s41598-020-78271-9>.
  30. Zhao HH, Liu YQ, Chen J. Screening acetylcholinesterase inhibitors from traditional Chinese medicines by paper-immobilized enzyme combined with capillary electrophoresis analysis. *J Pharm Biomed Anal.* 2020;190:113547. <https://doi.org/10.1016/j.jpba.2020.113547>.
  31. Li P, Ma XH, Dong YM, Jin L, Chen J. Alpha-Glucosidase immobilization on polydopamine-coated cellulose filter paper and enzyme inhibitor screening. *Anal Biochem.* 2020;605:113832. <https://doi.org/10.1016/j.ab.2020.113832>.
  32. Li X, Guan C, Gao X, Zuo X, Yang W, Yan H, Shi M, Li H, Sain M. High efficiency solar membranes structurally designed with 3D core-2D shell SiO<sub>2</sub>@amino-carbon hybrid advanced composite for facile steam generation. *ACS Appl Mater Interfaces.* 2020;12(31):35493–501. <https://doi.org/10.1021/acsami.0c10461>.
  33. Mallick I, Kirtania P, Szabo M, Bashir F, Domonkos I, Kos PB, Vass I. A simple method to produce *Synechocystis* PCC6803 biofilm under laboratory conditions for electron microscopic and functional studies. *PLoS One.* 2020;15(7):e0236842. <https://doi.org/10.1371/journal.pone.0236842>.
  34. Hu Q, Bu Y, Cao R, Zhang G, Xie X, Wang S. Stability designs of cell membrane cloaked magnetic carbon nanotubes for improved life span in screening drug leads. *Anal Chem.* 2019;91(20):13062–70. <https://doi.org/10.1021/acs.analchem.9b03268>.
  35. Chen WD, Zhao YL, Sun WJ, He YJ, Liu YP, Jin Q, Yang XW, Luo XD. “Kidney tea” and its bioactive secondary metabolites for treatment of gout. *J Agric Food Chem.* 2020;68(34):9131–8. <https://doi.org/10.1021/acs.jafc.0c03848>.
  36. Chen WD, Zhao YL, Dai Z, Zhou ZS, Zhu PF, Liu YP, Zhao LX, Luo XD. Bioassay-guided isolation of anti-inflammatory diterpenoids with highly oxygenated substituents from kidney tea (*Clerodendranthus spicatus*). *J Food Biochem.* 2020;44(12):e13511. <https://doi.org/10.1111/jfbc.13511>.

**Publisher's note** Springer Nature remains neutral with regard to jurisdictional claims in published maps and institutional affiliations.

Springer Nature or its licensor (e.g. a society or other partner) holds exclusive rights to this article under a publishing agreement with the author(s) or other rightsholder(s); author self-archiving of the accepted manuscript version of this article is solely governed by the terms of such publishing agreement and applicable law.